



# FLOW STRUCTURES GENERATED BY PRESSURE-CONTROLLED SELF-OSCILLATING REED VALVES

A. Z. TARNOPOLSKY, J. C. S. LAI AND N. H. FLETCHER\*

*Acoustics & Vibration Unit, School of Aerospace and Mechanical Engineering, University College,  
The University of New South Wales, Australian Defence Force Academy, Canberra 0200,  
Australia. E-mail: j.lai@adfa.edu.au*

(Received 17 April 2000, and in final form 20 November 2000)

The flow structures generated by a pressure-controlled self-oscillating valve are investigated both experimentally and numerically. Schlieren flow visualization experiments show that a stable vortex is developed downstream of the valve during the closing phase of the valve. During the opening phase of the valve, this vortex moves downstream and dissipates. An experimental study of the vortex interaction with a wedge and cylinder with different diameters shows that the vortex is a product of the large amplitude of the valve oscillation and does not significantly affect the valve behaviour. Finally, numerical modelling of the flow structures also supports the idea that the vortex development is an aerodynamic phenomenon accompanying a large amplitude of oscillation of pressure-controlled self-oscillating valves.

© 2001 Academic Press

## 1. INTRODUCTION

The sound producing mechanism in biological systems such as the vocal organs of birds and humans, and in musical instruments such as the brass and reed-woodwind families, may be simplified to various types of pressure-controlled self-oscillating valves.

It has proved helpful to classify the valves according to the effect of the upstream or downstream overpressure on the tendency of the valves to open further or to close. Thus, the valve will be called blown-closed when upstream overpressure tends to close the valve and downstream overpressure tends to open it. Similarly, the valve will be called blown-open when the upstream overpressure tends to open the valve and downstream overpressure tends to close it. Woodwind-type reeds are good examples of blown-closed valves while the human larynx and players lips in brass musical instruments can be considered as blown-open valves. Detailed explanation of the valve classification with descriptions of different types of pressure-controlled valves may be found in Fletcher [1].

There have been many studies of the behaviour of blown-closed valves in woodwind instruments where the air column of the instrument has a dominant influence. A more general study of the acoustics of valves of both types was carried out by Fletcher [2, 3],

\* Permanent address: Research School of Physical Science and Engineering, Australian National University, Canberra 0200, Australia.

while lip valves in brass instruments have been investigated by Elliott and Bowsher [4], Copley and Strong [5] and others. The behaviour of free reeds, as in harmoniums, has been studied by St. Hilaire *et al.* [6]. A summary of this work has been given by Fletcher and Rossing [7].

In aerodynamics, similar flow-induced vibration of bluff bodies is commonly referred to as a galloping instability [8]. The fundamental assumption of galloping analysis is that the fluid force is quasi-steady, i.e., the fluid force on the structure is determined solely by the instantaneous relative velocity. However, it has been found that if the body has instability in the range of Strouhal numbers  $0.1 < fD/U < 1.0$ , vortex shedding may also affect the body oscillation. Here,  $U$  is the flow velocity,  $f$  is the frequency of the body oscillation and  $D$  is the cross-flow width of the body, [8]. The vortex pattern behind bluff bodies known as the von Karman vortex street has been studied extensively in the past [9–12]. It has been found that an unbalanced periodic aerodynamic force affects the motion of the body.

In studying the acoustics of blown-closed valves, Hillarie *et al.* [6] did not find any connection between the valve oscillation and vortex shedding. This result is consistent with the fact that the reported Strouhal numbers based on the jet velocity, the reed natural frequency and the jet width, were less than 0.01. On the other hand, these authors also reported 10 times larger Strouhal numbers based on the frequency of the vortex formation.

The mechanism of self-oscillations of blown-open valves has been investigated recently [13]. Despite the geometric and dynamic complexities of systems of pressure-controlled valves, it is obvious that the mechanism of self-oscillation is based on oscillating pressure forces, induced by the valve motion. Even when the velocity of the jet through the valve is very small, jet separations on the valve edges cause a random turbulence of broad frequency spectrum to develop. The turbulence gives rise to unsteady pressure forces which excite random vibration of the valves of small amplitude of the order of the valve thickness. The small vibration is unstable and, when the pressure forces overcome damping, the valve vibration tends to grow rapidly to a large amplitude establishing self-oscillations with a frequency close to the valve resonance frequency. The amplitude of large oscillations was found to be of the order of the jet thickness. A quasi-steady approximation to time-varying flow [13] gives a good estimate of the threshold pressure of self-oscillations and shows that the valve oscillation frequency increases from its natural frequency with decreasing reservoir volume. A description of this large-amplitude behaviour necessarily involves proper treatment of the many non-linearities involved. In this instance, knowledge about flow structures would be a great advantage. It is therefore the purpose of the present study to investigate the flow structures generated by blown-open valves.

## 2. EXPERIMENTAL SET-UP AND TECHNIQUES

Details of the experimental arrangement are shown in Figure 1. The resonance reservoir was constructed from a heavy PVC pipe of inside diameter 101 mm. The upstream end of the pipe was terminated by a solid piston, the position of which could be changed to alter the reservoir volume. The downstream end of the pipe was closed by a face plate to which the valve was clamped.

The valve is essentially a thin brass flap which was cut from a flat brass sheet of thickness of either 0.15 mm or 0.33 mm. The valve is 28 mm in length and 53 mm in width. The relatively large width was chosen in order to give a good approximation to a two-dimensional flow through the valve. Also, an aluminium bar of mass 0.8 g was glued on the tip along the downstream side of the valve to prevent lateral oscillations, which could be observed stroboscopically in the absence of such stiffening. Application of the aluminium

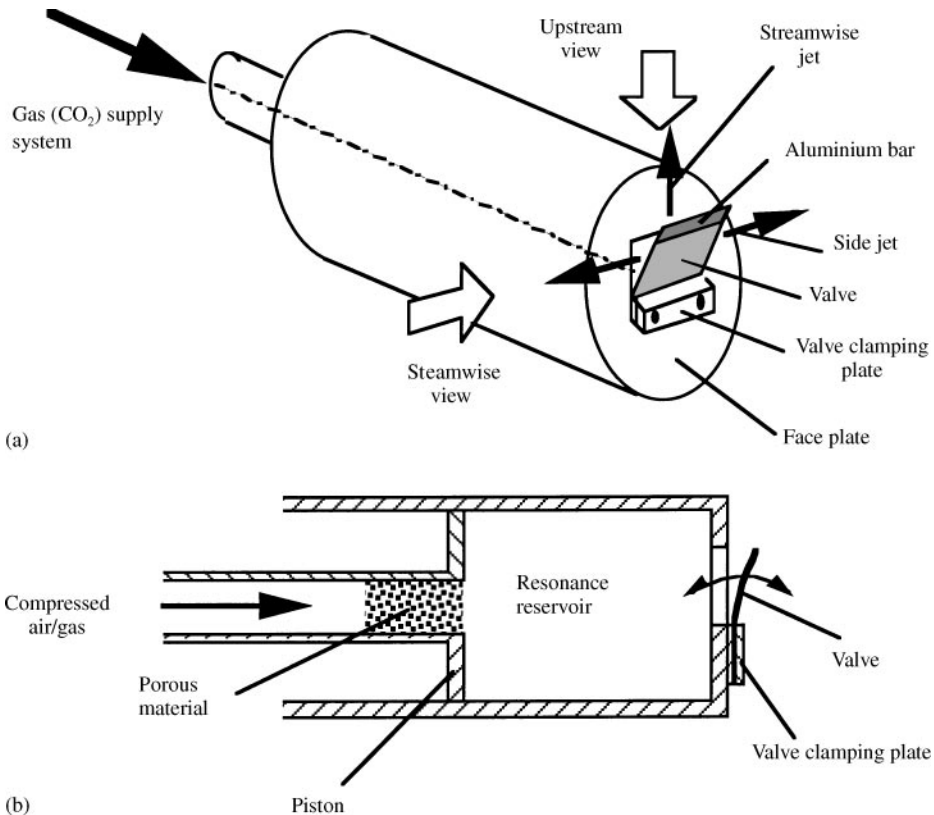


Figure 1. (a) Perspective view, and (b) sectional view, of the experimental set-up.

bar also reduced the valve oscillation frequency from 145 to 105 Hz, which was close to the natural frequency of the fundamental cantilever oscillation of the valve. The Q factor of the valve structural damping was changed by applying layers of sticky tape on both sides of the valve.

The aperture in the face plate under the valve was about 0.5 mm larger than the valve in both length and width, so that the valve was freely oscillating inside the aperture without striking against the face plate. The thickness of the plate was 4 mm. The offset gap between the stationary valve and the plate could be varied by inserting a thin shim sheet, and was normally fixed at either 0.5 mm or 1.0 mm.

In experiments to determine the threshold pressure for self-oscillating valves, compressed air was supplied to the reservoir through a long narrow tube terminating in a short coaxial pipe of diameter 37 mm filled with acoustically absorbent wool, as shown in Figure 1(b) [13]. This arrangement minimized turbulence in the reservoir while adequately defining its volume. The isolation effectiveness of the absorbing material was checked by using, in one experiment, a much narrower tube. Air was supplied from a high-pressure source through a reducing valve, and therefore constituted a high-impedance constant-flow source. During the experiments, the blowing pressure was varied between 30 and 1000 Pa giving Strouhal numbers within the range  $0.003 < St < 0.02$ . Here, the Strouhal numbers are based on the jet velocity, the valve oscillation frequency and the jet width.



To measure the amplitude of oscillation, the oscillating valve was illuminated by a stroboscope with the frequency tuned to reveal a slow motion of the valve. The travelling microscope was then used to focus on the valve tip at its upper and then lower positions. The distance between the two extreme positions was measured with a micrometer connected to the microscope. Repeated measurements gave an accuracy of  $\pm 0.02$  mm.

### 3. EXPERIMENTAL RESULTS

Figure 3 shows a set of Schlieren images of the flow field downstream of the oscillating valve in the streamwise view as defined in Figure 1 for a resonance volume ( $V$ ) of  $0.5\text{ l}$ , a blowing pressure ( $P_{BL}$ ) of  $310\text{ Pa}$ , a volume flow ( $U$ ) of  $2.1\text{ l}$  per second, a valve offset ( $X_o$ ) of  $1\text{ mm}$  and a frequency ( $f$ ) of  $110\text{ Hz}$ . The photographs were taken with the knife edge parallel to the face plate at every one-tenth of a period, with the zero phase taken to be the fully open position of the valve. The oscillating flap can be seen clearly in Figure 3(a)–3(c) and 3(g)–3(i). The most striking feature of the flow is a vortex downstream from the valve

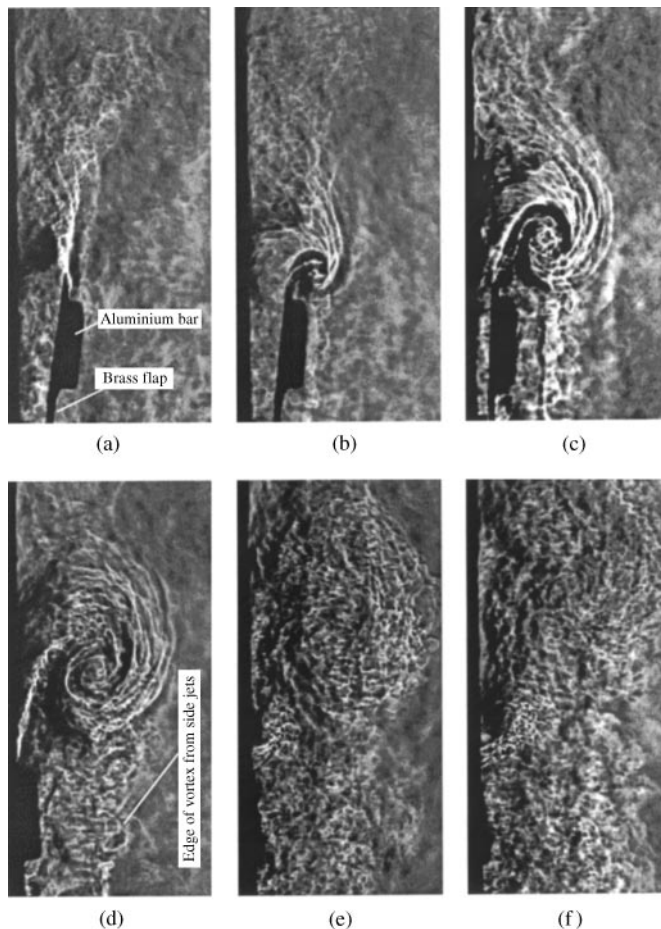


Figure 3. Streamwise view of vortex development during one period of the valve oscillation ( $P_{BL} = 310\text{ Pa}$ ,  $V = 0.5\text{ l}$ ,  $U = 2.1\text{ l/s}$ ,  $f = 110\text{ Hz}$ ,  $X_o = 1\text{ mm}$ ). (a)  $t/\tau = 1/10$ , (b)  $t/\tau = 2/10$ , (c)  $t/\tau = 3/10$ , (d)  $t/\tau = 4/10$ , (e)  $t/\tau = 5/10$ , (f)  $t/\tau = 6/10$ , (g)  $t/\tau = 8/10$ , (h)  $t/\tau = 9/10$ , (i)  $t/\tau = 10/10$ .

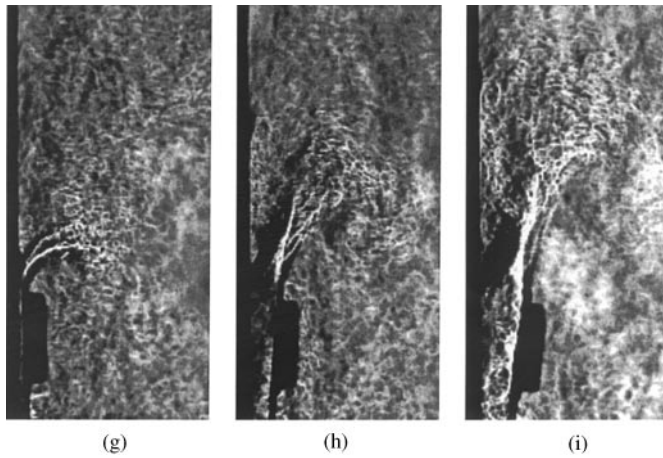


Figure 3. Continued

exit. The vortex is generated in a periodic fashion by the closing action of the valve, and appears to dissipate during the remainder of the cycle.

It can be seen from Figure 3b that the vortex starts to develop when the valve moves back from its fully open position where the acceleration is maximum. The vortex continues to grow until the valve is closed [Fig. 3(b, c)]. During this time, the vortex appears to be stable and remains localized in space. As the valve starts to open up again, this vortex moves downstream and diffuses into the surrounding air [Fig. 3(f, g)]. When the valve is nearly fully open, the vortex appears to be fully diffused and a new vortex is about to emerge [Figure 3(h)].

Schlieren images not shown here reveal a similar development of the vortex structures for a resonance volume of 1.6 l, a blowing pressure of 60 Pa, a volume flow of 0.65 l per second, a valve offset of 0.5 mm and a frequency of 133 Hz.

By measuring displacements of the vortex centre such as shown in Figure 3 and knowing the time separation between the Schlieren pictures, the magnitude of the vortex convective velocity [Figure 4(a)] and its direction [Figure 4(b)] were obtained for one period of the valve oscillation for two different experimental conditions. The magnitude of the vortex convective velocity was normalized here by the average jet velocity and its direction is specified by the angle it makes with the face plate.

It can be seen that despite a change of the blowing pressure from 60 to 310 Pa, the magnitude of the initial vortex velocity ( $U_c$ ) is approximately 20% of the average jet velocity [Figure 4(a)] and the direction of the vortex convection is very similar for both cases [Figure 4(b)]. However, it appears that the vortex for a lower blowing pressure ( $P_{BL} = 60$  Pa) starts to develop later (approximately 0.2 of a period of oscillation) than that of a higher blowing pressure ( $P_{BL} = 310$  Pa). The vortex for the lower blowing pressure convects faster and lasts longer before it begins to dissipate than that for the higher blowing pressure. This could be because when the blowing pressure is higher, the flow is more turbulent and as a result, the vortex dissipates earlier.

The experimental arrangement also allowed an upstream Schlieren view of the flow field to be observed (see Figure 1 for definition of the upstream view). The blowing pressure was 60 Pa and the knife edge in the optical set-up was also set parallel to the face plate. Figure 5 shows the Schlieren images of the upstream flow field. The large dark rectangle on the left lower side of the pictures is the valve clamping plate. The valve can be recognized on the

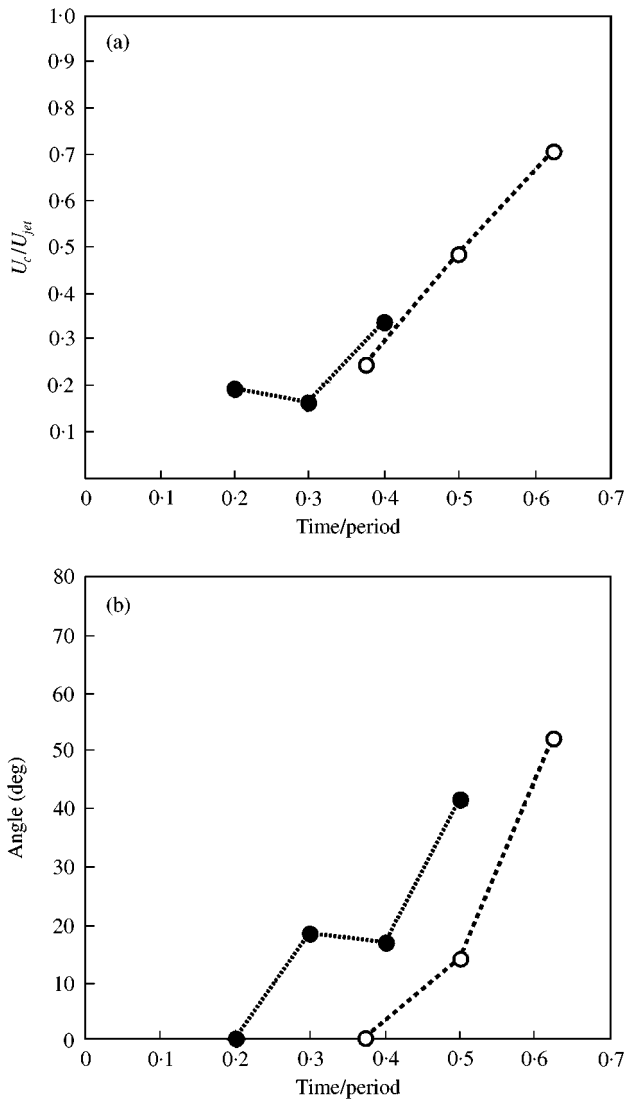


Figure 4. Variation of the vortex convective velocity during one period of the valve oscillation: (a) magnitude, (b) direction. -----○-----,  $P_{bt} = 60$  Pa,  $V = 1.6l$ ,  $X_o = 0.5$  mm; .....●.....,  $P_{bt} = 310$  Pa,  $V = 0.5l$ ,  $X_o = 1$  mm.

upper side of the clamping plate. The development of the side vortex can also be seen in Figure 5(c). By comparing Figures 3 and 5, we may conclude that the side vortex looks much weaker than the downstream vortex. However, the Schlieren technique depends on the deflection of a ray of light from its undisturbed path when it passes through a medium in which there is a density gradient. Thus, the image of the downstream vortex in Figure 4 is a superposition of the Schlieren effect along the valve width which is 53 mm, while the image of the side vortex is a superposition of the Schlieren effect along the valve length which is only 28 mm and varies in amplitude along this length. Thus, a visual weakness of the side vortex may probably be due to optical effects.

The downstream vortex can also be seen in Figure 5(b) and 5(c) behind the clamping plate as an edge parallel to the clamping plate. In a similar way, we can also see the side vortex on

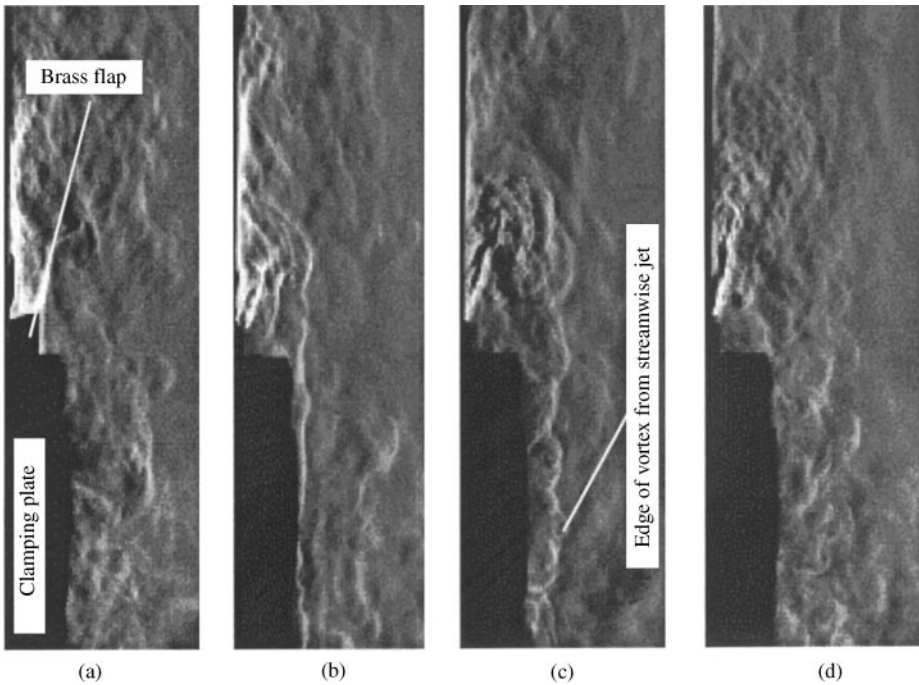


Figure 5. Upstream view of vortex development during one period of the valve oscillation ( $P_{BL} = 60$  Pa,  $V = 1.6$  l,  $U = 0.65$  l/s,  $f = 133$  Hz,  $X_o = 0.5$  mm). (a)  $t/\tau = 0$ , (b)  $t/\tau = 1/4$ , (c)  $t/\tau = 2/4$ , (d)  $t/\tau = 3/4$ .

Figures 3(b–f) as an edge parallel to the valve. By combining the observations of the flow field in Figures 3 and 5, we conclude that the flow through the valve exit aperture has an essentially two-dimensional nature, indicating that the vortex is indeed essentially a two-dimensional rolling large-scale structure with its axis parallel to the face plate.

In order to examine the effect of the blowing pressure on the vortex development, five experiments were performed with the reservoir volume kept at 1.6 l while the blowing pressure was increased from the threshold value up to nearly 4 times larger. The Schlieren pictures (see Figure 6) were taken at the time when the valve was nearly closed. It is rather surprising to find no difference in the position of the vortex centre in these pictures. The vortex is larger in size and looks more turbulent with larger blowing pressure but the centre of the vortex remains essentially in the same position. It seems that the vortex position does not depend on the blowing pressure and as a result it does not depend on the jet velocity, which is very interesting. Six other experiments were performed with different reservoir volumes. During the experiments, the blowing pressure was close to the threshold and Schlieren pictures were taken at the time when the valve was nearly closed. Despite differences in the threshold pressure and reservoir volume, no difference in the position of the vortex centre was observed.

In order to examine the role played by valve oscillations on the vortex development, Schlieren pictures (Figure 7) were taken with the blowing pressure below the threshold level of approximately 30 Pa. Under this condition, there are no oscillations of large amplitude. In order to enhance the two dimensionality of the streamwise jet [Figure 1(a)], side plates were installed to close off the side jets. It can be seen from Figure 7 that the jet turbulence increases producing more visible turbulence structures when the blowing pressure is raised.

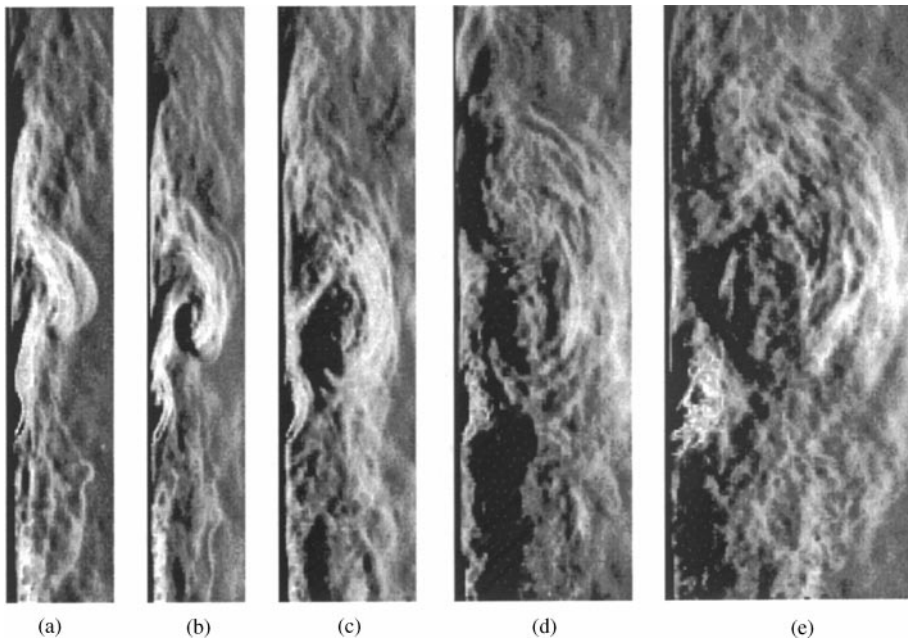


Figure 6. Structure of the downstream flow as the blowing pressure is increased above the threshold ( $V = 1.6l$ ,  $f = 110$  Hz,  $X_o = 0.5$  mm): (a) 30 Pa, (b) 40 Pa, (c) 60 Pa, (d) 80 Pa, (e) 110 Pa.

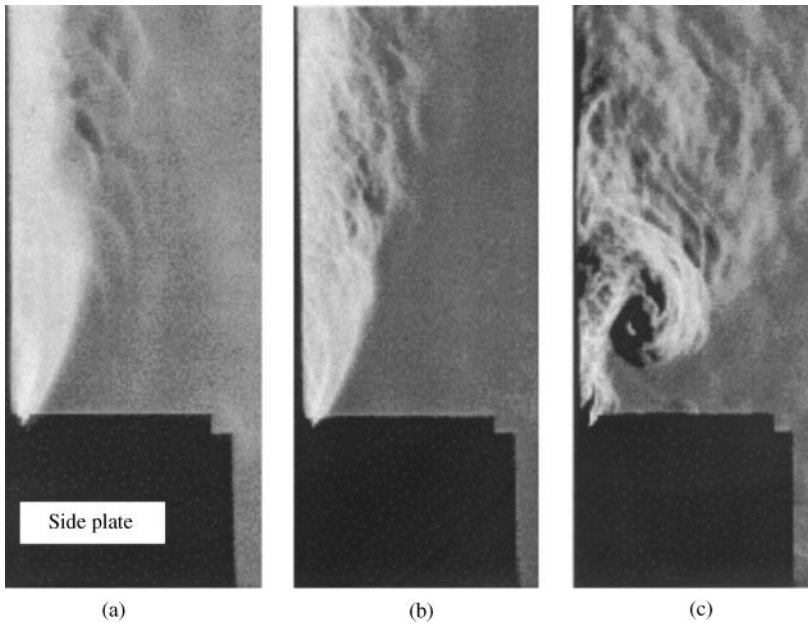


Figure 7. Structure of the downstream flow as blowing pressure is increased: (a) 20 Pa, (b) 30 Pa, (c) self-oscillation of the valve starts at 30 Pa and the blowing pressure jumps to 50 Pa. The valve is not oscillating in (a) and (b), but has begun to oscillate in case (c) ( $V = 1.6l$ ,  $f = 110$  Hz,  $X_o = 0.5$  mm).

Precise measurements of the valve motion using a stroboscope and a travelling microscope show that even at blowing pressures below the threshold, the valve still has a small oscillation with frequency close to its resonance frequency. At the threshold pressure of

approximately 30 Pa, the oscillation then becomes unstable and the amplitude of the oscillation grows rapidly to a limit cycle with a large amplitude. The photograph in Figure 7(c) was taken at half-period when the valve was nearly closed. In fact, the vortex starts to develop only when the valve has started to self-oscillate with a large amplitude.

However, the primary question still remains to be answered: does the vortex cause the valve to self-oscillate or do the valve oscillations caused by unsteady pressure fluctuations produce the vortex? To get an answer, we tried to suppress the vortex using cylinders with different diameters and using a wedge. The resulting flow patterns taken at the time when the valve was nearly closed for a blowing pressure of 40 Pa ( $V = 1.6l$ ,  $f = 110$  Hz,  $X_o = 0.5$  mm) are shown in Figures 8 and 9.

By introducing a small 3.15 mm diameter cylinder into the vortex centre, a periodic vortex flow was found moving along the wall, and a small stable vortex under the cylinder (see Figure 8(d)). When the cylinder was moved closer to the wall, the periodic vortex flow along the wall was suppressed but the stable vortex was only slightly shifted from the wall (see Figure 8(e)). It is interesting to note a "jelly-like" vortex behaviour in Figure 8b and 8c, when the cylinder was just touching the vortex. The vortex shows a similar behaviour when a cylinder with twice the diameter was introduced into the jet. It is concluded that the vortex development is not suppressed by introducing cylinders into the jet flow, even when the blowing pressure is close to the threshold value.

Figure 9 shows results of the Schlieren flow visualization of the vortex interaction with a wedge inserted into the flow. Figure 9(a) and 9(b) are similar to what was seen using the cylinder. When the wedge is far from the wall [Figure 9(a)], a stable vortex has been formed. As the wedge is moved closer to the wall [Figure 9(b)], this vortex moves under the wedge and a jet with periodic large-scale structures is emerging along the wall. When the wedge is moved even closer to the wall [Figure 9(c)], the stable vortex is suppressed and there are

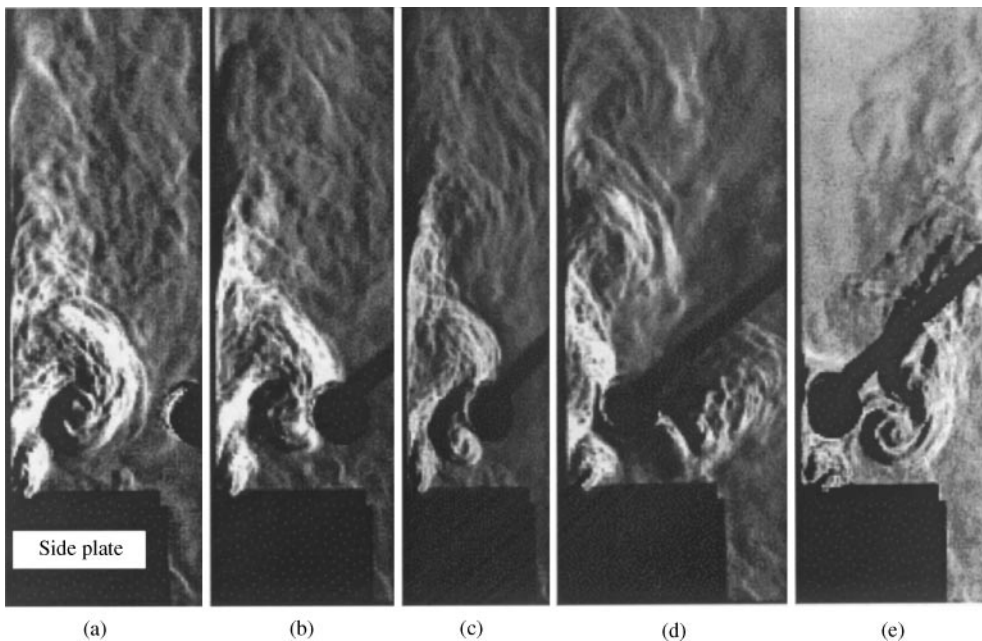


Figure 8. Vortex interaction with a cylinder 3.15 mm in diameter. The valve is oscillating in all cases. ( $V = 1.6l$ ,  $f = 110$  Hz,  $X_o = 0.5$  mm).

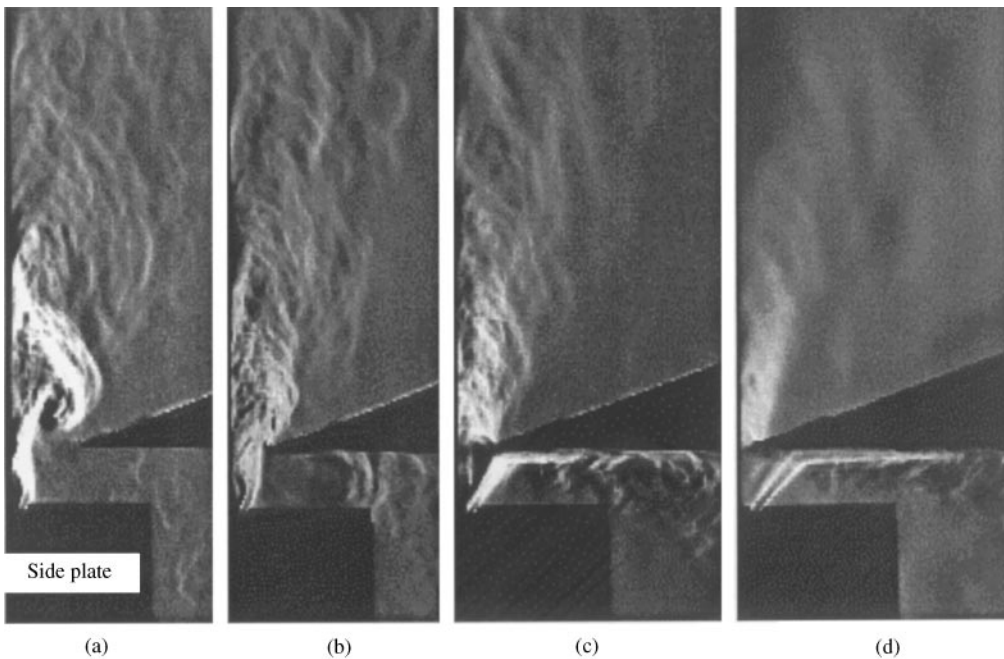


Figure 9. Vortex interaction with a wedge: from (a) to (c) valve is oscillating; in (d) valve oscillation is suppressed. ( $V = 1.6l$ ,  $f = 110$  Hz,  $X_o = 0.5$  mm).

two jets with periodic large-scale structures, one flowing along the wall and another running under the wedge. It should be noted that although the vortex is suppressed, the valve in Figure 9(c) has been observed to maintain large amplitude free self-oscillations. It can therefore be concluded that the vortex is not responsible for the valve self-oscillations. When the wedge was moved too close to the wall [Figure 9(d)], the valve self-oscillations were finally suppressed. Perhaps this could be attributed to the increase of the valve back pressure resulting in flow reductions through the valve.

In summary, it can be concluded that the vortex development is the result of valve free oscillations, rather than the other way round.

#### 4. NUMERICAL FLOW MODELLING

In order to confirm qualitatively that the vortex development is a common accompanying effect of a self-oscillating valve, numerical modelling of the flow structures behind a self-oscillating valve was carried out using a commercial CFD code FLUENT version 5.2 [16].

Since the unsteady flow behind self-oscillating valves is highly turbulent, the Reynolds-averaged Navier–Stokes transport equations were used to represent the mean flow quantities while the Reynolds stresses were modelled by employing the standard  $k$  (turbulence kinetic energy) –  $\varepsilon$  (turbulence dissipation rate) turbulence model [17]. Figure 10 shows a schematic of the computational domain, which is divided into two sub-domains: the upper stationary domain and the lower moving domain. The sub-domains were created using a structured quadrilateral grid with higher density and

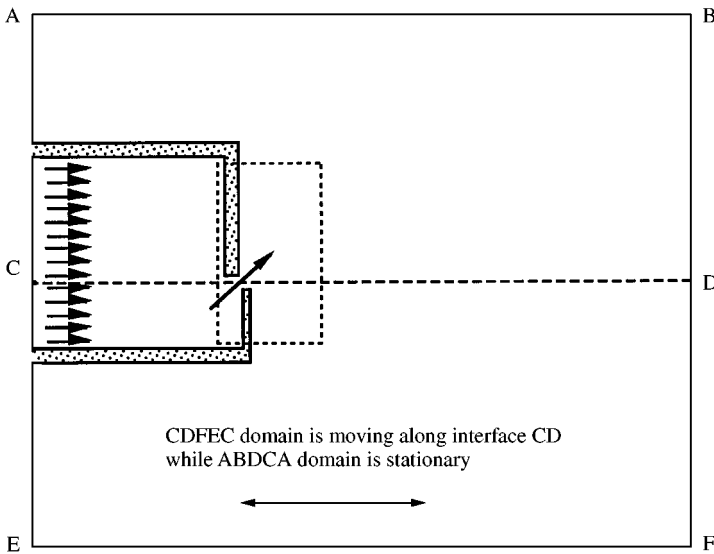


Figure 10. Schematic of the computational domain used for the numerical modelling of the flow structure generated by an oscillating valve. The horizontal broken line shows a periodic grid interface between the upper stationary face ABDCA and the lower moving face CDFEC. The broken line rectangle identifies the area of the domain where numerical results are compared with the experiment.

distribution of nodes in the mesh near the walls and along the CD line close to the valve aperture. The computational domain comprising a total number of 87 089 nodes covers a physical domain of 200 mm by 260 mm with the maximum valve aperture opening being 4 mm. Due to software limitations, it was not possible to model the cantilever motion of the valve with continuously varying velocity. Instead, the motion of the valve was modelled using a sliding mesh technique [16]. The period of the valve oscillation was divided into 10 time steps. Calculations were then carried out with a constant velocity for each time step using a second order upwind finite difference scheme in space and a second order implicit finite difference scheme in time. In order to check the accuracy of the solution, the period of the valve oscillation was divided into 22 time steps and calculations were repeated. It has been found that there is no significant difference between calculations obtained by 10 time steps and those by 22 time steps.

Contours of vorticity magnitude were used to display the results of the calculation. Defined as the curl of the velocity vector, vorticity represents a measure of the rotation in the flow field. The closed contours of vorticity give an estimate of the position of a vortex in the flow field.

Figure 11 shows the result of calculations at various phases during one period of oscillation of the valve. Despite simplifications and limitations of the numerical model, the result of the calculation shows good similarity with the experiment. With respect to the vortex development and dissipation, the vorticity contours show that the vortex grows stronger and larger during the closing phase of the valve [Figure 11 (a, b)]. From the end of the closing phase of the valve to the opening phase of the valve motion, the vorticity contours separate from the valve, becoming closed [Figure 11(c)], moving downstream [Figure 11(d)] and dissipating along the way [Figure 11(e)]. At the start of the closing phase of the valve, a vortex begins to emerge at the edge of the valve [Figure 11(f)]. Calculations made with a coarser grid of 27 292 nodes show no real qualitative differences in the spatial

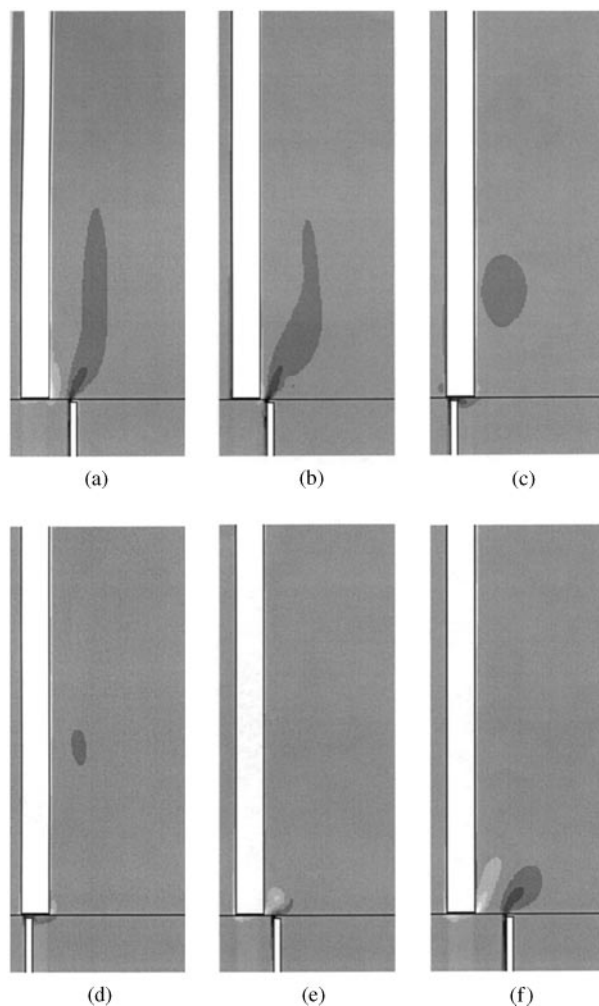


Figure 11. Vorticity contours from numerical modelling of the flow structure generated by an oscillating valve at different phases of the oscillation ( $P_{BL} = 310$  Pa,  $f = 110$  Hz). (a)  $t/\tau = 1/10$ , (b)  $t/\tau = 2/10$ , (c)  $t/\tau = 4/10$ , (d)  $t/\tau = 6/10$ , (e)  $t/\tau = 8/10$ , (f)  $t/\tau = 10/10$ .

development and dissipation of the vortex. It is interesting to note that, as in the flow visualization experiments, the moving edge of the valve is identified as the source of the vorticity development.

## 5. CONCLUSIONS

Flow structures downstream of a pressure-controlled self-oscillating valve have been investigated using the Schlieren technique. It has been found that a stable vortex is developed during the closing phase of the valve. As the valve starts to open up, this vortex moves downstream and eventually dissipates.

Schlieren flow visualization shows that the vortex cannot be suppressed by inserting cylinders with different diameters into the vortex and the valve maintains large amplitude

self-oscillations. On the other hand, experiments with a wedge show that even when the vortex is suppressed, the valve can still maintain large amplitude self-oscillations provided that the back pressure due to the presence of the wedge is not too high as to severely reduce the flow through the valve. These results indicate that the vortex itself should therefore be considered to be a product of the large amplitude oscillations rather than the cause of self-oscillation. Numerical modelling also supports the idea that the vortex development is simply an aerodynamic phenomenon accompanying a large amplitude oscillation.

#### ACKNOWLEDGMENTS

This work is part of a programme supported by a grant from the Australian Research Council.

#### REFERENCES

1. N. H. FLETCHER 1993 *Journal of the Acoustical Society of America* **93**, Part 1, 2172–2180. Autonomous vibration of simple pressure-controlled valve in gas flows.
2. N. H. FLETCHER 1979 *Acustica* **43**, 63–72; erratum in **50**, 115–159 (1982). Excitation mechanisms in woodwind and brass instruments.
3. N. H. FLETCHER, R. K. SILK and L. M. DOUGLAS 1982 *Acustica* **50**, 155–159. Acoustic admittance of air-driven reed generators.
4. S. J. ELLIOT and J. M. BOWSER 1982 *Journal of Sound and Vibration* **83**, 181–217. Regeneration in brass wind instruments.
5. D. C. COPLEY and W. J. STRONG 1996 *Journal of the Acoustical Society of America* **99**, 1219–1226. A stroboscopic study of lip vibrations in a trombone.
6. A. O. ST HILAIRE, T. A. WILSON and G. S. BEAVERS 1971 *Journal of Fluid Mechanics* **49**, Part 4, 803–816. Aerodynamic excitation of the harmonium reed.
7. N. H. FLETCHER and T. D. ROSSING 1998 *The Physics of Musical Instruments*. New York: Springer-Verlag.
8. R. D. BLEVINS 1977 *Flow-induced Vibration*. New York: Van Nostrand Reinhold Company.
9. B. R. MUNSON, D. F. YOUNG and T. H. OKIISHI 1998 *Fundamentals of Fluid Mechanics*. New York: John Wiley & Sons, Inc.
10. S.-S. CHEN 1987 *Flow-induced Vibration of Circular Cylindrical Structures*. Berlin: Springer-Verlag.
11. A. ROSHKO 1955 *Journal of Aeronautical Science* 124–132. On the wake and drag of bluff bodies.
12. H. OERTEL, JR. 1990 *Annual Review of Fluid Mechanics* **22**, 539–564. Wakes behind blunt bodies.
13. A. TARNOPOLSKY, N. H. FLETCHER and J. C. S. LAI 2000 *Journal of the Acoustical Society of America* **108**, 400–406. Oscillating reed valves—an experimental study.
14. D. W. HOLDER and R. J. NORTH 1963 *Notes on Applied Science* **31**, (London) Schlieren methods.
15. W. MERZKIRCH 1987 *Flow Visualization*. New York: Academic Press.
16. Fluent Incorporated 1998 *FLUENT 5 User's Guide*. Lebanon: Centerra Resource Park.
17. B. E. LAUNDER and D. B. SPALDING 1972 *Lectures in Mathematical Models of Turbulence*. London, U.K.: Academic Press.